*Advances in Reliability, Safety and Security, Part 6 – Kołowrocki, Magryta-Mut (eds.)*
*© 2024 Polish Safety and Reliability Association, Gdynia, ISBN 978-83-68136-18-0 (printed), ISBN 978-83-68136-05-0 (electronic)*

**Advances in Reliability, Safety and Security**

ESREL 2024
Monograph Book Series

# A Risk Assessment Model Of Complex Systems Based On Evidential Reasoning Rule With Dependent Evidence

Shuai-Wen Tang[a], You Cao[b], Hai-Yue Yu[a]

[a]*National University of Defense Technology, Changsha, China*
[b]*Rocket Army Sergeant School, Qingzhou, China*

**Abstract**

In this paper, an innovative model called evidential reasoning rule with dependent evidence (ERR-DE) is proposed for the risk assessment of complex systems under uncertainties. A general risk assessment indicator system is established, and the risk indicators are modeled and described as evidence under the discernment of framework (FoD). The evidence is unified by the transformation matrix, and the evidence reliability and dependence index of evidence are explicitly measured. The ERR-DE model forms a multi-information fusion framework, where multiple pieces of evidence with different weights, reliabilities and dependence indexes are aggregated to establish the relationship between risk indicators and system risk. A parameter optimization model is constructed, where all subjective evidential parameters can be learned through the idea of maximizing expectations. The proposed model is applied to assess the risk of a laser gyroscope.

*Keywords*: risk assessment, inferential modeling, evidenital reasoning rule, uncertainty, evidence dependence

## 1. Introduction

Risk assessment aims to quantitatively assess the possible degree of impact or loss caused by a risk event before or after the event, which is of great significance (Kuzior et al., 2023) (Deng et al., 2023.). Recent years have witnessed rapid developments and applications of risk assessment in different fields, such as aeronautics and aerospace, critical infrastructure, industrial automation and control, etc.

Existing risk assessment methods can be divided into three categories, involving the knowledge-based method, the data-driven method, and the hybrid information-based method. The knowledge-based method directly establishes a systematic risk assessment model through mechanism analysis and expert knowledge, which has strong transparency and interpretability, including the analytic hierarchy process method, Petri net, Fault tree, etc. However, when the system mechanism is complex, it is difficult to obtain the expert knowledge and the assessment result may have strong subjective uncertainties, which is not conducive to improving the assessment accuracy. The data-driven method does not require precise acquisition of the analytical model of the system, and a risk assessment model can be established based on statistical data, including artificial neural network, TOPSIS method, deep learning, etc. However, this method needs to acquire accurate data and relies on large samples, which lacks interpretability and traceability. In comparison, the hybrid information-based method can combine qualitative knowledge and quantitative data to effectively assess the risk level of complex systems using small samples, including Bayesian network, fuzzy comprehensive evaluation, belief rule base, evidential reasoning rule (ERR). This method provides a sound idea for the risk assessment of complex systems.

As a typical hybrid information-based method, the ERR forms a generalized probabilistic reasoning scheme to achieve multi-source information fusion, which extends traditional Bayes' rule and Dempster-Shafer rule (Yang and Xu, 2013). It constructs a so-called discernment of framework (FoD) to model various uncertainties, under which a piece of evidence can be described as the belief distribution. By using the ERR, the system inputs can be transformed to multiple evidence with weight and reliability, which can be aggregated to build a bridge between system inputs and output. With the advancement of evidence theory, the ERR has been widely applied in the risk assessment of complex systems (Gizem et al. 2023). In the ERR, however, the FoD of evidence should strictly correspond to the FoD of reasoning results. Thus, when assessing the system risk, all risk indicators and the risk assessment result should be limited in the same FoD. This is incredibly difficult since different experts can provide different types and quantities of assessment grades according to the system design principle and standard. Besides, the ERR requires all the evidence to be independent of each other from theoretical aspect, which tends to be idealized due to the coupling of system structure. Even though the maximum likelihood evidential reasoning (MAKER) framework has been proposed to aggregate interdependent evidence, it requires joint probabilities and marginal probabilities under all combinations, resulting in exponential computational complexity (Yang and Xu, 2017) (Zhang et al. 2023). Most importantly, with the increase of the number of risk indicators, experts will find themselves in a dilemma to accurately give all evidential parameters due to incomplete or limited knowledge. This can greatly increase the subjective uncertainty of the risk assessment.

Based on the above analysis, the paper aims to introduce a new risk assessment model for complex systems, referred to as evidential reasoning rule with dependent evidence (ERR-DE). The main contents are as follows:

(1) The rule/utility-based equivalence transformation technique is used to acquire evidence, and the evidence unification method is proposed based on the concept of transformation matrix.

(2) To better express the subjective judgment and personal preferences of experts, the evidence weight is described in interval form and further optimized. A calculation method of evidence reliability is proposed based on static and dynamic reliability, and a discounting factor is defined.

(3) A calculation method of dependence index between evidence is proposed, and the relative total dependence coefficient (RTDC) is defined using the distance correlation method.

(4) A risk assessment model called ERR-DE is proposed to aggregate all the evidence information, where the risk probability and the risk degree are used to measure the system risk from discrete and continuous aspects, respectively.

(5) To alleviate the subjective uncertainty brought by experts, a parameter optimization model is constructed, which is conducive to improving the risk assessment accuracy.

(6) The effectiveness of ERR-DE model is illustrated and verified by a case study.

## 2. Proposed risk assessment model

As for a certain system, the risk degree can be measured by the so-called risk indicators, and the corresponding observation data can be monitored by sensors. Suppose there are $L$ risk indicators denoted by $x_1, x_2, \cdots, x_L$, which can be monitored by $L$ different sensors. Then, a typical risk assessment indicator system can be constructed as Figure 1.

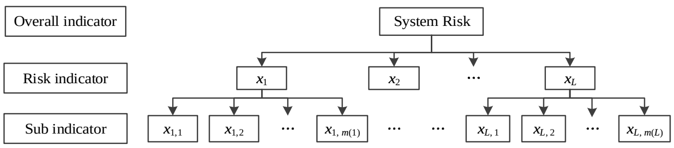


Fig. 1. General risk assessment indicator system.

In Figure 1, the number of sub indicators as $m(l)$ can be further refined according to the actual situation, where $l \in [1, m(L)]$ and $m(L)$ depends on $L$. Within time interval $T$, the observation data matrix of indicator $x_i$ at time instant $t$ can be represented by $\mathbf{Z}_i(t) = [x_i(t-T) \quad x_i(t-T+1) \quad \cdots \quad x_i(t)]$. Each indicator can provide a piece of evidence at $t$, denoted by $e_i(t)$. Correspondingly, the evidence weight and evidence reliability can be denoted by $w_i$ and $r_i(t)$ respectively, $0 \le w_i, r_i(t) \le 1$. The evidence reliability is time-varying, consisting of static reliability $r_i^s$ and dynamic reliability $r_i^d(t)$. The dependence index between $e_i(t)$ and all evidence is $d_i(t)$. Thus, the ERR-DE-based risk assessment model can be constructed.

### 2.1. Evidence acquisition method and unification method

Suppose the FoD of risk indicator $x_i$ is $\Theta_i = \{H_{i,1}, H_{i,2}, \cdots, H_{i,n(i)}\}$, where $H_{i,k}$ is the $k$th risk grade of $x_i$, and $i \in [1, L]$ and $k \in [1, n(i)]$. $n(i)$ is related to $i$. The referential value of $H_{i,k}$ is $h_{i,k}$. If $x_i$ is a benefit indicator, there is $h_{i,1} < h_{i,2} < \cdots < h_{i,n(i)}$. If $x_i$ is a cost indicator, there is $h_{i,1} > h_{i,2} > \cdots > h_{i,n(i)}$. Suppose the observation data of $x_i$ at time instant $t$ is $x_i(t)$. Without loss of generality, suppose $h_{i,k} < x_i(t) < h_{i,k+1}$, where $k, k+1 \in [1, n(i)]$. The rule/utility-based equivalence transformation technique can be used to acquire evidence (Yang, 2001), shown as follows:

$$\beta_{i,k}(t) = \frac{h_{i,k+1} - x_i(t)}{h_{i,k+1} - h_{i,k}} \tag{1}$$

$$\beta_{i,k+1}(t) = 1 - \beta_{i,k}(t) \tag{2}$$

$$\beta_{i,j}(t) = 0; j \neq k, k+1 \text{ and } j \in [1, n(i)]. \tag{3}$$

In the above equations, $\beta_{i,k}(t)$, $\beta_{i,k+1}(t)$ and $\beta_{i,j}(t)$ are belied degrees that $x_i(t)$ is assessed to risk grade $H_{i,k}$, $H_{i,k+1}$ and $H_{i,j}$ respectively. Obviously, there is $\sum_{j=1}^{n(i)} \beta_{i,j}(t) = 1$. Based on the above method, a piece of evidence can be profiled by the following belief distribution:

$$e_i(t) = \left\{\left(H_{i,j}, \beta_{i,j}(t)\right); j \in [1, n(i)]\right\} \tag{4}$$

Suppose the FoD of risk assessment result is $\Theta = \{H_1, H_2, \cdots, H_n\}$, and a piece of evidence under $\Theta$ can be profiled by:

$$e(t) = \left\{\left(H_p, \beta_p(t)\right); p \in [1, n]\right\} \tag{5}$$

where $\beta_p(t)$ is the belief degree to risk grade $H_p$. As mentioned in Section 1, the FoD of evidence may differ from the FoD of result. This means that $\Theta_i$ is not completely equivalent to $\Theta$ in terms of the number and type of assessment grades. To unify different FoDs, the concept of transformation matrix is introduced to establish the mapping relationship between $\Theta_i$ and $\Theta$, shown as follows:

$$\mathbf{A}_i = \begin{bmatrix} \alpha_{1,1} & \alpha_{2,1} & \cdots & \alpha_{n,1} \\ \alpha_{1,2} & \alpha_{2,2} & \cdots & \alpha_{n,2} \\ \vdots & \vdots & \ddots & \vdots \\ \alpha_{1,n(i)} & \alpha_{2,n(i)} & \cdots & \alpha_{n,n(i)} \end{bmatrix} \tag{6}$$

where $\mathbf{A}_i$ is the transformation matrix with a dimension of $n(i) \times n$. Each row of $\mathbf{A}_i$ can be denoted by an "IF-THEN" rule as $R_{i,k}$. $R_{i,k}$ means that "IF $x_i$ is $H_{i,k}$, THEN $\{(H_1, \alpha_{1,k}), (H_2, \alpha_{2,k}), \cdots, (H_n, \alpha_{n,k})\}$, with $0 \leq \alpha_{p,k} \leq 1$ and $\sum_{p=1}^{n} \alpha_{p,k} \leq 1$". Here, all elements of $\mathbf{A}_i$ are given by experts.

Suppose the belief degree matrix of $e_i$ is $\boldsymbol{\beta}_i = \left[\beta_{i,1}, \beta_{i,2}, \cdots, \beta_{i,n(i)}\right]$, and the belief degree matrix of $e$ is $\mathbf{B} = [\beta_1, \beta_2, \cdots, \beta_n]$. According to (6), we have

$$\mathbf{B} = \boldsymbol{\beta}_i \cdot \mathbf{A}_i \tag{7}$$

Based on the above analysis, all evidence can be unified to the same FoD as $\Theta$. To better understand the transformation matrix, here is an example of human health risk screening. Suppose the health level of a human is divided into three grades as "Healthy", "Sub Healthy", and "Unhealthy". Thus, the FoD of risk assessment result can be denoted by $\Theta = \{\text{Healthy}, \text{Sub Healthy}, \text{Unhealthy}\}$. The health risk can be measured by two indicators as body temperature and blood pressure. According to relevant inspection standards, suppose "body temperature" provides a piece of evidence under $\Theta_1 = \{\text{High}, \text{Medium}, \text{Low}\}$, and "blood pressure" provides a piece of evidence under $\Theta_2 = \{\text{Very High}, \text{High}, \text{Medium}, \text{Very Low}, \text{Low}\}$. As such, the FoD of evidence is different from the FoD of assessment results. To effectively synthesize two pieces of evidence, the transformation matrix should be used to establish the mapping relationship between $\Theta_1$, $\Theta_2$ and $\Theta$. In summary, the transformation matrix serves as a set of "IF-THEN" rules, which can achieve consistency in the assessment framework.

### 2.2. Calculation methods of evidence weight and reliability

Since different experts may assign different weights to a risk indicator, to effectively deal with such subjective uncertainty and fully leverage the role of experts in empowerment, the interval is employed to describe the evidence weight. For example, if there are $M$ experts, denoted by $E_1, E_2, \cdots, E_M$, assigning different evidence weights as $w_{i,1}, w_{i,2}, \cdots, w_{i,M}$ to $x_i$, all weights can be arranged in ascending order. Without loss of generality, suppose there is $w_{i,1} < w_{i,2} < \cdots < w_{i,M-1} < w_{i,M}$. The interval weight of $x_i$ can be given by $[w_{i,2}, w_{i,M-1}]$ with the maximum and minimum weights deleted.

As the observation data of risk indicators can be influenced by environmental noises, the evidence reliability is introduced to measure the data quality. In the context of sensor, the evidence reliability is composed of static reliability and dynamic reliability of sensor (Tang et al. 2022). The static reliability $r_i^s$ is an objective attribute of sensor, which a fixed value. It can be determined by the factory parameters of sensor or assesed by experts (Fan and Zuo, 2006). In comparison, the dynamic reliability $r_i^d(t)$ is a subjective attribute of sensor, which can be obtained by the distance-based method (Zhao et al. 2018). Thus, the evidence reliability can be calculated as follows:

$$r_i(t) = \alpha r_i^s + (1-\alpha) r_i^d(t) \quad (8)$$

where $\alpha \in [0,1]$ is a discounting factor, reflecting the contribution of static reliability and dynamic reliability to evidence reliability. It is normally given by experts. If $\alpha = 0$, there is $r_i(t) = r_i^d(t)$. If $\alpha = 1$, there is $r_i(t) = r_i^s$.

### 2.3. Calculation method of dependence index

Affected by such factors as system structure coupling and mechanism correlation, the risk indicators may not be strictly independent of each other. Hence, it is necessary to consider the correlation of indicators. Due to the unequal reliability of different risk indicators, the evidence reliability can be used to determine the aggregation sequence (Yager, 2009) (Zhang et al. 2023). This indicates that the higher the reliability of an indicator is, the higher its aggregation sequence will be. In this paper, the dependence index of evidence is defined as RTDC using the distance correlation method.

As for two pieces of evidence $e_i(t)$ and $e_j(t)$ at time instant $t$, and the evidence reliabilities are $r_i(t)$ and $r_j(t)$ respectively. The relative aggregation sequence $Seq_{i,j}(t)$ can be determined as follows:

$$Seq_{i,j}(t) = \begin{cases} Seq_i(t) < Seq_j(t), & if \ r_i(t) > r_j(t) \\ Seq_{i,j}(t-1), & if \ r_i(t) = r_j(t) \\ Seq_i(t) > Seq_j(t), & otherwise \end{cases} \quad (9)$$

where $Seq_i(t)$ and $Seq_j(t)$ refer to the aggregation sequence of $e_i(t)$ and $e_j(t)$ respectively.

Given two observation data matrices $\mathbf{Z}_i(t)$ and $\mathbf{Z}_j(t)$, the distance correlation coefficient of $e_i(t)$ and $e_j(t)$ can be calculated as follows (Székely et al. 2007):

$$C\left(\mathbf{Z}_i(t), \mathbf{Z}_j(t)\right) = \begin{cases} \frac{v^2(\mathbf{Z}_i(t), \mathbf{Z}_j(t))}{\sqrt{v^2(\mathbf{Z}_i(t)) v^2(\mathbf{Z}_j(t))}}, & if \ v^2(\mathbf{Z}_i(t)) v^2\left(\mathbf{Z}_j(t)\right) > 0 \\ 0, & if \ v^2(\mathbf{Z}_i(t)) v^2\left(\mathbf{Z}_j(t)\right) = 0 \end{cases} \quad (10)$$

where $v^2(\mathbf{Z}_i(t), \mathbf{Z}_j(t))$ is the empirical distance covariance between $\mathbf{Z}_i(t)$ and $\mathbf{Z}_j(t)$. $v^2(\mathbf{Z}_i(t))$ and $v^2(\mathbf{Z}_j(t))$ denote the empirical distance variance of $\mathbf{Z}_i(t)$ and $\mathbf{Z}_j(t)$ respectively.

Without loss of generality, suppose the aggregation sequence of $e_1(t), e_2(t), \cdots, e_L(t)$ is $\{1,2,\cdots,L\}$. The correlation matrix $\mathbf{C}$ can be given by:

$$\mathbf{C} = \begin{bmatrix} C(\mathbf{Z}_1(t), \mathbf{Z}_1(t)) & 0 & \cdots & 0 \\ C(\mathbf{Z}_2(t), \mathbf{Z}_1(t)) & C(\mathbf{Z}_2(t), \mathbf{Z}_2(t)) & \ldots & 0 \\ \vdots & \vdots & \ddots & \vdots \\ C(\mathbf{Z}_L(t), \mathbf{Z}_1(t)) & C(\mathbf{Z}_L(t), \mathbf{Z}_2(t)) & \ldots & C(\mathbf{Z}_L(t), \mathbf{Z}_L(t)) \end{bmatrix} \quad (11)$$

The total dependence degree of $e_i(t)$ can be calculated as follows:

$$Tdd_i(t) = \sum_{j=1}^{i} C\left(\mathbf{Z}_i(t), \mathbf{Z}_j(t)\right) \quad (12)$$

The dependence index between $e_i(t)$ and all evidence is $d_i(t)$, i.e., the RTDC value, which can be calculated as follows:

$$\overline{d_i}(t) = \frac{1/Tdd_i(t)}{\sum_{j=1}^{L} 1/Tdd_j(t)} \quad (13)$$

$$d_i(t) = \frac{\overline{d_i}(t)}{\max\{\overline{d_i}(t)\}}, i \in [1, L] \quad (14)$$

It can be concluded from the above equations that $d_i(t) \in [0,1]$ and the larger the value of $d_i(t)$, the stronger the independence between $e_i(t)$ and all evidence. If $d_i(t) = 1$, $x_i$ is regarded as independent of other evidence.

### 2.4. ERR-DE-based risk assessment model

According to the above analysis, the ERR-DE model is proposed in this section. As for a piece of evidence $e_i(t)$ profiled by (5) with weight and reliability of $w_i$ and $r_i(t)$, in the FoD as $\Theta = \{H_1, H_2, \cdots, H_n\}$, the hybrid probability mass can be calculated as follows:

$$m_{i,\theta}(t)=\begin{cases}0, & \theta=\emptyset\\ \overline{w_i}d_i(t)\beta_{i,\theta}(t), & \theta\subseteq\Theta\ and\ \theta\neq\emptyset\\ 1-\overline{w_i}d_i(t), & \theta=P(\Theta)\end{cases} \tag{15}$$

where $\emptyset$ denotes the empty set. $\overline{w_i}$ is the hybrid weight, and $\overline{w_i}=w_i/(1+w_i-r_i(t))$. $P(\Theta)$ is the power set of $\Theta$, which is composed of $2^n$ subsets of $\Theta$. It can describe local and global ignorance in the assessment profiled by:

$$P(\Theta)=\{\emptyset,\{H_1\},\{H_2\},\cdots,\{H_n\},\{H_1,H_2\},\cdots,\{H_1,H_2,\cdots,H_{n-1}\},\Theta\} \tag{16}$$

As for two pieces of evidence $e_i(t)$ and $e_j(t)$ profiled by (4), the evidence combination based on ERR-DE can be expressed as:

$$\beta_{e(2),\theta}(t)=\begin{cases}0, & \theta=\emptyset\\ \frac{m_{e(2),\theta}(t)}{\sum_{\varphi\subseteq\Theta}m_{e(2),\varphi}(t)}, & \theta\subseteq\Theta\ and\ \theta\neq\emptyset\end{cases} \tag{17}$$

$$m_{e(2),\theta}(t)=\sum_{\phi\cap\psi=\theta}m_{i,\phi}(t)m_{j,\psi}(t);\ \ \phi,\psi\subseteq\Theta \tag{18}$$

where $\beta_{e(2),\theta}(t)$ is the combined belied degree of risk grade $\theta$ from $e_i(t)$ and $e_j(t)$, $\theta\subseteq\Theta$. $m_{e(2),\theta}(t)$ represents the unnormalized combined probability mass of $\theta$. $m_{i,\phi}(t)$ and $m_{j,\psi}(t)$ denote hybrid probability masses of $e_i(t)$ and $e_j(t)$ assigned to risk grades $\phi$ and $\psi$ respectively.

As for $L$ pieces of evidence $e_1(t),e_2(t),\cdots,e_L(t)$, equations (17) and (18) can be recursively used $(L-1)$ times to generate the final risk assessment result, which can be profiled by the following belief distribution:

$$S_{e(L)}(t)=\left\{\left(\theta,\beta_{e(L),\theta}(t)\right);\theta\subseteq\Theta\right\} \tag{19}$$

where $\beta_{e(L),\theta}(t)$ is the final combined belied degree of risk grade $\theta$, $\theta\subseteq\Theta$. Obviously, there is local and global ignorance in $S_{e(L)}(t)$ since $\theta$ is not just a single subset. Thus, it is necessary to map $S_{e(L)}(t)$ to real probabilities of single subsets $H_p$ for further assessment and decision (He et al. 2023). The calculation method is given by:

$$P_{H_p}(t)=\sum_{\theta\subseteq\Theta}\beta_{e(L),\theta}(t)\frac{|H_p\cap\theta|}{\theta};p\in[1,n] \tag{20}$$

where $P_{H_p}(t)$ is the risk probability that the complex system is at the risk grade $H_p$ at time instant $t$.

Suppose the utility of $H_p$ is $u(H_p)$, the expected utility of the system can be calculated as follows:

$$RD(t)=\sum_{p=1}^{n}P_{H_p}(t)u(H_p) \tag{21}$$

where $RD(t)\in[0,1]$ can quantitatively measure the risk degree of system. Compared with discrete risk grades $H_p$ in $\Theta$, $RD(t)$ is a continuous variable that can illustrate the risk degree more effectively. A larger $RD(t)$ closer to 1 reflects a higher risk, while a lower $RD(t)$ closer to 0 reveals a lower risk.

It should be noted that the proposed ERR-DE model forms a nonlinear multiple information fusion scheme. Research on the nonlinear characteristics of ER approach can be found in (Yang and Xu, 2002). In addition, in the ERR-DE model, the individual risk indicators forming the overall risk indicator do not necessarily need to be independent in practice.

### 2.5. Proposed parameter optimization model

In the ERR-DE model, there are several parameters given by experts, including evidence weights, referential values of risk grades in different FoDs, and the transformation matrix. This will cause strong subjective uncertainty in the risk assessment result. As mentioned in Subsection 2.2, the evidence weight belongs to an interval $[w_{i,2},w_{i,M-1}]$, which will make $RD(t)$ fluctuate within a certain range. Suppose the expected risk degree is $RD$, and the observed result is $RD(t)$. To alleviate the subjective uncertainty of evidential parameters, a parameter optimization model can be established by maximizing the likelihood of expected risk degree as follows:

$$min\ \Gamma=\frac{1}{t}\sum_{\tau=1}^{t}[RD(\tau)-RD]^2 \tag{22}$$

s.t.

$$\begin{cases}0\leq\alpha_{p,k}\leq 1\ and\ \sum_{p=1}^{n}\alpha_{p,k}\leq 1\\ w_i^-<w_i<w_i^+\\ h_{i,k}^-<h_{i,k}<h_{i,k}^+\end{cases} \tag{23}$$

where $w_i^+$ and $w_i^-$ denote the upper and lower bounds of evidence weight $w_i$. $h_{i,k}^+$ and $h_{i,k}^-$ represent the upper and lower bounds of referential value $h_{i,k}$ in initial FoDs. The goal is to minimize $\Gamma$, and the expected risk degree $RD$ is given based on the expert judgment.

## 3. Case study

In this section, the risk assessment of a type of laser gyroscope is conducted to show the implementation process of the proposed ERR-DE model. According to the mechanism analysis, the risk of laser gyroscope is mainly related to drift coefficient and light intensity. Thus, the risk assessment indicator system can be constructed as Figure 2.

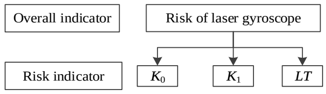


Fig. 2. Risk assessment indicator system of laser gyroscope.

In Figure 2, $K_0$ and $K_1$ denote the zero-item and first-item drift coefficients of the laser gyroscope, respectively. $LT$ is the light intensity. In the experiment, the gravitational acceleration of the experimental site is 9.8015 m/s$^2$. A total of 100 sets of data are collected, as shown in Figure 3.

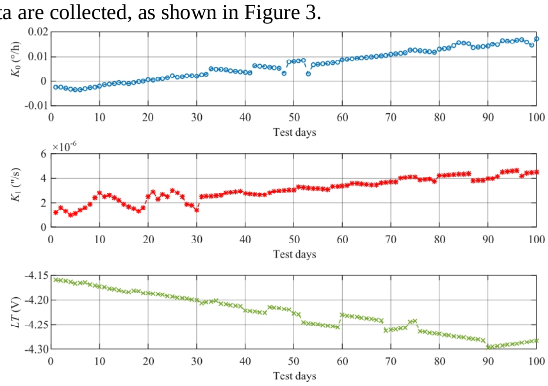


Fig. 3. Observation data of $K_0$, $K_1$ and $LT$.

### 3.1. Acquisition of evidence and determination of initial parameters

Based on factory parameters and expert knowledge, the referential grades and referential values of risk indicators are listed in Table 1 and Table 2.

Table 1. Referential grades and referential values of drift coefficients.

| Referential grade | Small | Medium | Large |
|---|---|---|---|
| $K_0$ (°/h) | [-0.03, -0.01] | [-0.01, 0.01] | [0.01, 0.03] |
| $K_1$ ("/s) | [0, 3×10$^{-6}$] | [3×10$^{-6}$, 7×10$^{-6}$] | [7×10$^{-6}$, 1.2×10$^{-5}$] |

Table 2. Referential grades and referential values of light intensity.

| Referential grade | Very weak | Weak | Medium | Strong | Very Strong |
|---|---|---|---|---|---|
| $LT$ (V) | [-4.32, -4.28] | [-4.28, -4.24] | [-4.24, -4.2] | [-4.2, -4.16] | [-4.16, -4.12] |

According to Table 1, the FoD of drift coefficients can be denoted by $\Theta_1 = \{\text{Small}, \text{Medium}, \text{Large}\}$. The unit of light intensity is V in Table 2, which is the output of an A/D conversion circuit. As such, the FoD of light intensity can be denoted by $\Theta_2 = \{\text{Very weak}, \text{Weak}, \text{Medium}, \text{Strong}, \text{Very strong}\}$. By using the rule/utility-based equivalence transformation technique, all the observation data can be transformed to evidence. For example, in Figure 3, the observation data of $K_0$ on the first day is -0.0023°/h. If $h_{1,1} = -0.02°/\text{h}$ and $h_{1,2} = 0°/\text{h}$, based on (1)-(3), the evidence can be generated by:

$$\beta_{1,1}(1) = \frac{h_{1,2}-x_1(1)}{h_{1,2}-h_{1,1}} = \frac{0-(-0.0023)}{0-(-0.02)} = 0.1150, \quad \beta_{1,2}(1) = 1-\beta_{1,1}(1) = 0.8850, \quad \beta_{1,3}(1) = 0 \tag{24}$$

Thus, the evidence acquired from $K_{0X}$ on the first day can be profiled by:

$$e_1(1) = \{(\text{Small}, 0.1150), (\text{Medium}, 0.8850), (\text{Large}, 0)\} \tag{25}$$

Limited by page number, the detailed results will not be presented here. To obtain the evidence weight, we invite 5 experts to participate in empowerment. Also, the FoD of risk assessment result is set as $\Theta = \{\text{Low}, \text{Medium}, \text{High}\}$. Obviously, there is inconsistency among $\Theta_1$, $\Theta_2$ and $\Theta$. Thus, the evidence in $\Theta_1$ and $\Theta_2$ should be transformed to $\Theta$. The initial evidential parameters are given as follows for illustration:

Table 3. Initial parameters of risk indicators.

| Risk indicator | $K_0$ | $K_1$ | $LT$ |
|---|---|---|---|
| Interval weight | [0.8, 0.9] | [0.75, 0.85] | [0.75, 0.85] |
| Static reliability | 0.95 | 0.85 | 0.9 |
| Discounting factor | | 0.8 | |

Table 4. Referential values of risk grades in $\Theta$.

| Risk grade | Low | Medium | High |
|---|---|---|---|
| Referential value | [0, 0.4] | [0.4, 0.7] | [0.7, 1] |

$$\mathbf{A}_1 = \begin{bmatrix} 0.25 & 0.5 & 0.25 \\ 1 & 0 & 0 \\ 0.8 & 0.2 & 0 \end{bmatrix} \; and \; \mathbf{A}_2 = \begin{bmatrix} 1 & 0 & 0 \\ 0.8 & 0.2 & 0 \\ 0.25 & 0.25 & 0.5 \end{bmatrix} \; and \; \mathbf{A}_3 = \begin{bmatrix} 0.8 & 0.2 & 0 \\ 1 & 0 & 0 \\ 0.8 & 0.2 & 0 \\ 0.6 & 0.4 & 0 \\ 0.4 & 0.3 & 0.3 \end{bmatrix} \tag{26}$$

As such, all evidence can be unified to the same FoD as $\Theta$. By using the distanced-based method, the dynamic reliability of each risk indicator can be calculated. Based on (8), the evidence reliability is depicted in Figure 4.

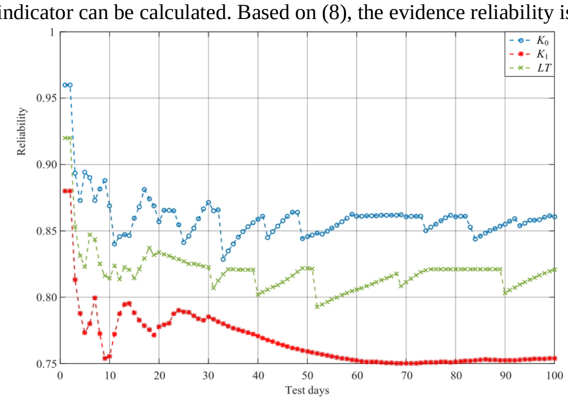


Fig. 4. Reliability of risk indicators.

Based on (9)-(14) and Figures 3-4, the significance level is set as 5%, and the RTDC value of each risk indicator can be obtained. It is calculated that $d_1 = 1$, $d_2 = 0.3496$, $d_3 = 0.5106$.

### 3.2. Parameter optimization

Based on (22), the objective function can be established, and the constraints can be obtained from Tables 1-4.

$$min\ \Gamma = \frac{1}{100}\sum_{\tau=1}^{100}[RD(\tau) - RD]^2 \tag{27}$$

In this section, the initial values of all evidential parameters are set as the average values of corresponding intervals. Using the Fmincon Function in Matlab Optimization Tool, the above optimization problem can be solved. The optimal transformation matrices are as (28), and other optimal evidential parameters are listed in Tables 5-8.

$$\mathbf{A}_1^* = \begin{bmatrix} 0.56 & 0.26 & 0.18 \\ 0.87 & 0.08 & 0.05 \\ 0.05 & 0.13 & 0.82 \end{bmatrix} \quad and \quad \mathbf{A}_2^* = \begin{bmatrix} 0.56 & 0.25 & 0.19 \\ 0.25 & 0.28 & 0.47 \\ 0.34 & 0.32 & 0.34 \end{bmatrix} \quad and \quad \mathbf{A}_3^* = \begin{bmatrix} 0.22 & 0.29 & 0.49 \\ 0.19 & 0.24 & 0.57 \\ 0.30 & 0.41 & 0.29 \\ 0.73 & 0.17 & 0.10 \\ 0.40 & 0.31 & 0.29 \end{bmatrix} \tag{28}$$

Table 5. Optimal referential values of drift coefficients.

| Referential grade | Small | Medium | Large |
|---|---|---|---|
| $K_0$ (°/h) | -0.0230 | 0.0009 | 0.0132 |
| $K_1$ ("/s) | $1.9\times10^{-6}$ | $4.2\times10^{-6}$ | $9.5\times10^{-6}$ |

Table 6. Optimal referential values of light intensity.

| Referential grade | Very weak | Weak | Medium | Strong | Very Strong |
|---|---|---|---|---|---|
| $LT$ (V) | -4.302 | -4.265 | -4.216 | -4.185 | -4.137 |

Table 7. Optimal weight of risk indicators.

| Risk indicator | $K_0$ | $K_1$ | $LT$ |
|---|---|---|---|
| Optimal weight | 0.85 | 0.80 | 0.80 |

Table 8. Optimal referential values of risk grades in Θ.

| Risk grade | Low | Medium | High |
|---|---|---|---|
| Optimal Referential value | 0.0157 | 0.5564 | 0.9826 |

Based on Subsection 2.4, the risk probabilities of laser gyroscope relative to different risk grades can be obtained using the optimized ERR-DE model, shown as Figure 5.

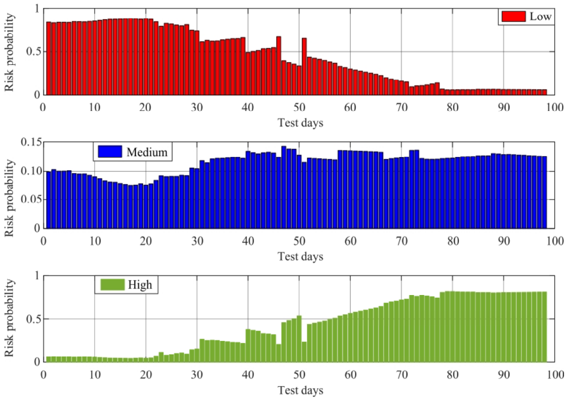


Fig. 5. Risk probability of laser gyroscope.

It can be seen from Figure 5 that as the number of test days increases, the risk probability of grade "Low" decreases dramatically from roughly 0.88 to 0.06. For grade "Medium", the risk probability fluctuates around 0.10, and the amplitude is relatively gentle. In comparison, the risk probability of grade "High" increases rapidly from about 0.04 to 0.82. This also means that the likelihood of risks occurring with laser gyroscope is increasing. It should be noted that the trend of risk probability change for three risk grades is not strictly monotonically increasing or decreasing. The potential reason contains two aspects. On the one hand, in the process of probability reasoning, the risk grade corresponding to the highest risk probability is generally considered as the actual risk state in which the laser gyroscope is in. The overall trend Figure 5 shows that the overall severity of risks associated with laser gyroscopes is increasing. On the other hand, the performance degradation process of laser gyroscopes is not continuous. Due to the internal fault-tolerant mechanism of laser gyroscope, when the performance degradation reaches a certain level, there will be a slight decrease in the risk probability. However, this does not affect the overall trend of risk changes.

To further reveal the overall changes in the risk degree of laser gyroscope, the risk assessment results between the optimized ERR-DE model and the expected result are compared, as shown in Figure 6. According to Figure 6, the mean square error (MSE) value between the optimal assessment result by ERR-DE model and the expected result is 0.0079. This demonstrates that the optimized ERR-DE model can well describe the changes in the risk degree of laser gyroscope. Overall, the risk degree increases from approximately 0.10 to 0.87. As mentioned in Subsection 2.4, an increase in $RD(t)$ means an increase in risk degree, which is also consistent with Figure 5. Therefore, the effectiveness of the proposed ERR-DE model is validated.

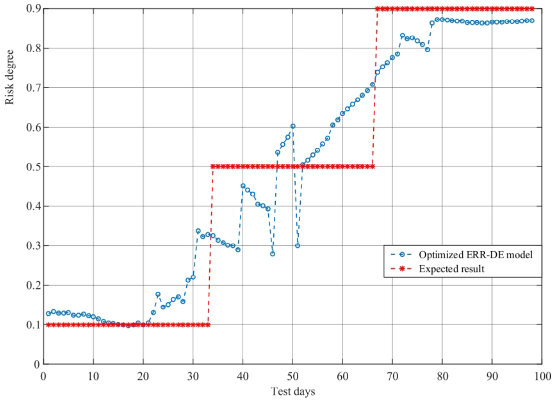


Fig. 6. Comparison between the ERR-DE model and the expected result.

### 3.3. Comparison with classical ER approach

In this subsection, a classical ER approach called the ERR model is used for comparison to further verify the effectiveness of the proposed ERR-DE model. In the ERR model, the inconsistency of FoD is not considered, and the dependence index of evidence is ignored. To unify the FoD of evidence, we set $\Theta_2 = \{\text{Weak}, \text{Medium}, \text{Strong}\}$, and the referential values of $LT$ are listed in Table 9. Other parameters are consistent with the ERR-DE model.

Table 9. Referential grades and referential values of light intensity in ERR scheme.

| Referential grade | Weak | Medium | Strong |
|---|---|---|---|
| $LT$ (V) | [-4.3, -4.25] | [-4.25, -4.2] | [-4.2, -4.15] |

Using the Fmincon Function in Matlab Optimization Tool, the ERR model can be optimized. The risk assessment results generated by different ER models are compared in Figure 7.

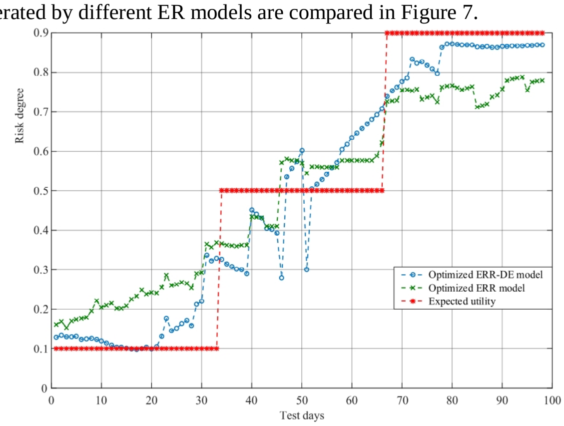


Fig. 7. Comparison among different ER models.

It can be seen from Figure 7 that the MSE value between the optimal assessment result by ERR model and the expected result is 0.0172. Compared with ERR model, the assessment accuracy of ERR-DE model increases by about 54.7%. Due to the incomplete consideration of uncertainty in ERR model, its risk assessment accuracy is relatively low. On the one hand, the inconsistency of FoD is not considered in the ERR model, increasing the uncertainty in setting initial values. On the other hand, in the ERR model, all evidence is independent of each other in default, which is difficult to match with reality. Hence, the above comparative study also shows the effectiveness of the proposed ERR-DE model.

## 4. Conclusion

In this paper, an ERR-DE-based risk assessment model for complex systems is briefly introduced with a case study. It constitutes a multi-source information fusion framework, which can make full use of qualitative knowledge and quantitative data to analyze the system risk under various uncertainties. Based on the establishment of a general risk assessment indicator system, all risk indicators are transformed to evidence under different FoDs. The transformation matrix is introduced to unify different evidence to the same FoD. The subjective and objective evidential parameters are considered, with the dependence index of evidence measured by RTDC. All evidence is aggregated by the ERR-DE model to assess the system risk, which is measured by the risk probability and the risk degree, respectively. Moreover, the parameter uncertainty is well alleviated by a parameter optimization model.

In view of the achieved new results, the future work should be focused on the sensitivity analysis or robustness analysis of the risk assessment model. Besides, the ability of ERR-DE model to deal with large-scale evidence information needs to be further investigated.

## Acknowledgements

The paper presents the results of the work granted by Polish Safety and Reliability Association. This paper is supported in part by the National Natural Science Foundation of China under Grant 62303474 and Shandong Provincial Natural Science Foundation of China under Grant ZR2023QF010.

## References

Deng, S., Zhang, J, T., Wu, D., et al. 2023. A quantitative risk assessment model for distribution cyber-physical system under cyberattack. IEEE Transactions on Industrial Informatics 19(3), 2899-2908.

Fan, X, F., Zuo, M, J. 2006. Fault diagnosis of machines based on D-S evidence theory. Part 1: D-S evidence theory and its improvement. Pattern Recognition Letters 27(5): 366-376.

Gizem, E., Sukru, I, S., Emre, A., et al. 2023. Operational risk assessment of ballasting and de-ballasting on-board tanker ship under FMECA extended Evidential Reasoning (ER) and Rule-based Bayesian Network (RBN) approach. Reliability Engineering and System Safety 231, 108975.

He, R, F., Zhang, L, M., Tiong, R, L, K. 2023. Flood risk assessment and mitigation for metro stations: An evidential-reasoning-based optimality approach considering uncertainty of subjective parameters. Reliability Engineering and System Safety 238, 109453.

Kuzior, A., Yarovenko, H., Brożek, P,. et al. 2023. Company cybersecurity system: assessment, risks and expectations. Production Engineering Archives 29(4), 379-392.

Székely, G, J., Rizzo, M, L., Bakirov, N, K. 2007. Measuring and testing dependence by correlation of distances. The Annals of Statistics 35(6), 2769-2794.

Tang, S, W., Zhou, Z, J., Hu, C, H., et al. 2022. A new evidential reasoning rule-based safety assessment method with sensor reliability for complex systems. IEEE Transactions on Cybernetics 52(5), 4027-4038.

Yager, R, R. 2009. On the fusion of non-independent belief structures. International Journal of General Systems 38(5), 505-531.

Yang, J, B. 2001. Rule and utility based evidential reasoning approach for multiattribute decision analysis under uncertainties. European Journal of Operational Research 131(1), 31-61.

Yang, J, B., Xu, D, L. 2002. Nonlinear information aggregation via evidential reasoning in multiattribute decision analysis under uncertainty. IEEE Transactions on Systems, Man, and Cybernetics-Part A: Systems and Humans 32(3), 376-393.

Yang, J, B., Xu, D, L. 2013. Evidential reasoning rule for evidence combination. Artificial Intelligence 205, 1-29.

Yang, J, B., Xu, D, L. 2017. Inferential modelling and decision making with data. In Automation and Computing (ICAC), 2017 23rd International Conference on IEEE. https://doi.org/10.23919/IConAC.2017.8082048.

Zhang, P., Zhou, Z, J., Tang, S, W., et al. 2023. On the evidential reasoning rule for dependent evidence combination. Chinese Journal of Aeronautics 36(5), 306-327.

Zhao, F, J., Zhou, Z, J., Hu, C, H., et al. 2018. A new evidential reasoning-based method for online safety assessment of complex systems. IEEE Transactions on Systems, Man, and Cybernetics: Systems 48(6): 954-966.